

Preparation and characterization of $\text{Ni}_{0.8}\text{Mn}_{0.2}\text{Fe}_2\text{O}_4$ nanoparticles synthesized by thermal decomposition of $\text{Ni}_{0.8}\text{Mn}_{0.2}\text{Fe}_2(\text{PhAc})_3(\text{N}_2\text{H}_4)_5$



Chemistry

KEYWORDS : Nanoparticles, TG-DTA, XRD, SEM, HRTEM

Sinduja CR

Department of Chemistry, Kongunadu Arts and Science College, Coimbatore, Tamilnadu, India-641 029.

Kalpanadevi K

Department of Chemistry, Kongunadu Arts and Science College, Coimbatore, Tamilnadu, India-641 029.

Manimekalai R

Department of Chemistry, Kongunadu Arts and Science College, Coimbatore, Tamilnadu, India-641 029.

ABSTRACT

Ni-Mn ferrite nanoparticles have been synthesized using carboxylate precursor via thermal decomposition route. The prepared precursor $\text{Ni}_{0.8}\text{Mn}_{0.2}\text{Fe}_2(\text{PhAc})_3(\text{N}_2\text{H}_4)_5$ was characterized by hydrazine, metal analyses, infrared spectral and thermal analyses. Using appropriate annealing conditions, $\text{Ni}_{0.8}\text{Mn}_{0.2}\text{Fe}_2\text{O}_4$ nanoparticles of average size 13 nm were synthesized by thermal treatment of the precursor. The nanoparticles were characterized by using X-ray diffraction (XRD), Scanning Electron Microscope (SEM), High Resolution Transmission Electron Microscope (HRTEM) and Selected Area Electron Diffraction (SAED) techniques. The details of synthesis and characterizations of the nanoparticles are reported in this paper.

INTRODUCTION

Nanotechnology has gained enormous interest in the past 20 years. They are interesting due to their fascinating size-dependent. Transition metal nanoparticles have drawn huge attention due to the unique optical, electronic, magnetic, thermal, mechanical, chemical properties and magnetic properties derived from their nanosizes and uniform size distribution [1]. Magnetic ferrite nanoparticles can be used in heat transfer devices, drug delivery systems and medical diagnostics because of their high electrical resistivity, chemical stability, mechanical hardness and reasonable cost [2-4]. Typically nanosized spinel ferrite particles have attracted considerable interest, and efforts continue to investigate them for their technological applications in the microwave industries, disk recording, refrigeration systems, electrical devices, ferrofluids, etc. [5-7]. Increased application of ferrites has led to the development of many chemical methods which includes ceramic technique [8], coprecipitation [9], microemulsion [10], micelle and hydrothermal methods [11] and sol-gel process [12]. The size and shape of the ferrite particles are dependent on the synthesis process.

The growing interest during the past decade is essentially due to the possibility of reduction in manufacturing cost on account of energy savings, shorter processing times and improved product uniformity and yields. Thermal treatment is an exciting new field with enormous potential for synthesizing new materials and novel nanostructures. Precursor used in the thermal treatment is more important for the synthesis of fine nanoparticles. Hydrazine derivatives of metal carboxylates serve as precursors to produce fine particle oxide materials. Hydrazine is not only used as a fuel, it also supports for combustion in the reduction of particle size [13,14]. Many such thermal decomposition methods are employed for the synthesis of metal and mixed metal oxides using metal carboxylate and carboxylato-hydrazinates complexes of oxalate [15], formate [16], acetate and propionate [17] malonate, succinate and itaconates [18,19], maleate and tartrate [20,21], malate [22] and fumarate [23-25] have been studied

Thermal decomposition method is an easy and fast process which yields high-purity, homogenous, crystalline oxides in a short time and with less energy. We deal in this paper with the preparation of Ni-Mn ferrites using the inorganic precursor $\text{Ni}_{0.8}\text{Mn}_{0.2}\text{Fe}_2(\text{PhAc})_3(\text{N}_2\text{H}_4)_5$ and detailed structural characterization of these particles.

Preparation of nickel manganese ferrous phenylacetate hydrazinate $\text{Ni}_{0.8}\text{Mn}_{0.2}\text{Fe}_2(\text{PhAc})_3(\text{N}_2\text{H}_4)_5$

Nickel manganese ferrous phenylacetate hydrazinate was pre-

pared by mixing an aqueous solution containing the requisite quantity of phenylacetic acid and hydrazine hydrate to the solution containing the stoichiometric amount of freshly prepared ferrous sulphate solution mixed with nickel nitrate hexahydrate and manganese acetate tetrahydrate with constant stirring. The complex is precipitated slowly, which is kept for sometime. A yellow coloured precipitate thus obtained was filtered off, washed with ethanol, dried with diethyl ether and then stored in a vacuum desiccator.

Preparation of $\text{Ni}_{0.8}\text{Mn}_{0.2}\text{Fe}_2\text{O}_4$ nanoparticles by thermal decomposition method

The precursor complex $\text{Ni}_{0.8}\text{Mn}_{0.2}\text{Fe}_2(\text{PhAc})_3(\text{N}_2\text{H}_4)_5$ thus prepared was taken in a clean silica crucible and heated gently at the starting and strongly when the decomposition starts. As a result the precursor complex was completely decomposed to ferrite $\text{Ni}_{0.8}\text{Mn}_{0.2}\text{Fe}_2\text{O}_4$.

CHARACTERIZATION

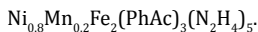
All the chemicals used were of pure commercial grade. The hydrazine content in the precursor was determined by volumetric analysis using (0.25M) KIO_3 as the titrant under Andrews' condition [26]. The percentage of nickel, manganese and iron in the precursor was estimated by the standard methods given in the Vogel's textbook [26]. The metal content in the sintered oxide sample were also determined by EDX.

Infrared analysis of the precursor complex $\text{Ni}_{0.8}\text{Mn}_{0.2}\text{Fe}_2(\text{PhAc})_3(\text{N}_2\text{H}_4)_5$ was carried out on a Perkin-Elmer model 597 spectrophotometer using KBr pellets. The thermal measurements (TG- DSC) are performed using a Netzsch SDT Q600 device from RT to 1000°C in nitrogen atmosphere. The crystalline phases are identified by XRD powder methods using a Seifert X-ray diffractometer (CuK α radiation). The morphology of the as synthesized nano particle was determined by a Scanning Electron Microscope (SEM, Philips XL-30) which is equipped with an Energy-Dispersive X-ray spectrometer (EDX). High Resolution Transmission Electron Microscopy (HR-TEM) images and Selected Area Electron Diffraction Pattern (SAED) were collected using a Jeol Jem 2100 advanced analytical electron microscope to determine the shape and size of the nanoparticles.

RESULTS AND DISCUSSION

Characterization of precursor complex $\text{Ni}_{0.8}\text{Mn}_{0.2}\text{Fe}_2(\text{PhAc})_3(\text{N}_2\text{H}_4)_5$ spectral and structural study

The observed percentage of hydrazine (21.43), nickel (20.95), manganese (4.68) and iron (47.07) are very well in agreement with the calculated values of 21.72, 20.00, 4.70 and 47.80 respectively. From the above data the chemical formula for the precursor complex is tentatively assigned as



The infra-red spectrum of the precursor complex shows three bands in the range of 3181 cm^{-1} - 3295 cm^{-1} due to N-H stretching frequencies. The separation of asymmetric and symmetric ($\nu_{\text{asymm}} - \nu_{\text{sym}}$) carboxylate stretching of 205 cm^{-1} indicates the unidentate coordination [27] of carboxylate ions. The N-N stretching frequency of hydrazine moieties was observed at 977 cm^{-1} indicating their bidentate bridging nature [28]. The IR data thus reveals that the nickel manganese ferrous phenylacetate hydrazinate complex is formed.

Thermal analysis

The nickel manganese ferrous complex shows a multistep decomposition in nitrogen atmosphere (Fig. 1). Initially it lost two hydrazine molecules exothermally in the temperature range from room temperature to $158\text{ }^\circ\text{C}$, and then it eliminates three hydrazine molecules exothermally in the temperature from $158 - 182\text{ }^\circ\text{C}$. TG curve from $182 - 545\text{ }^\circ\text{C}$ can be attributed to the decarboxylation of the dehydrazinated precursor. DTA curve showed exothermic peak in this region $499\text{ }^\circ\text{C}$ is due to decarboxylation. $\text{Ni}_{0.8}\text{Mn}_{0.2}\text{Fe}_2(\text{PhAc})_3(\text{N}_2\text{H}_4)_5$ precursor loss thermo gravimetrically from room temperature to $700\text{ }^\circ\text{C}$ to yield $\text{Ni}_{0.8}\text{Mn}_{0.2}\text{Fe}_2\text{O}_4$ as the final product.

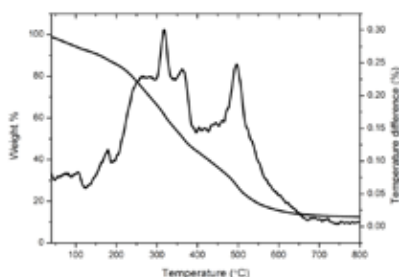


Fig.1 TG-DTA of the precursor
Characterization of $\text{Ni}_{0.8}\text{Mn}_{0.2}\text{Fe}_2\text{O}_4$ Nanoparticles

Phase analysis

The phase and its purity were confirmed by powder X-ray diffraction (XRD). Fig. 2 shows the peak position and the relative intensity of all the diffraction peaks which well matched with standard powder diffraction data. No impurity peak was observed, indicating the formation of high purity crystalline $\text{Ni}_{0.8}\text{Mn}_{0.2}\text{Fe}_2\text{O}_4$ nanoparticles. All the peaks coincident with a typical single-phase cubic spinel structure. The broadening nature of the XRD peaks indicates that the crystallite size of the as-prepared sample is within nanometer scale. Considering the more intense peak, the average crystallite size was calculated by Scherrer formula [29,30], $D = (0.94\lambda)/B \cos(\theta)$, where, λ —Wave length of X-rays, B —Full width at half maximum, θ —The diffraction angle.

The Scherrer formula analysis shows that the average diameter of the grain sizes of $\text{Ni}_{0.8}\text{Mn}_{0.2}\text{Fe}_2\text{O}_4$ is 13 nm . The X-ray diffraction data such as d-values and lattice parameter of 'as synthesized' $\text{Ni}_{0.8}\text{Mn}_{0.2}\text{Fe}_2\text{O}_4$ was found to match closely with the reported values [31,32].

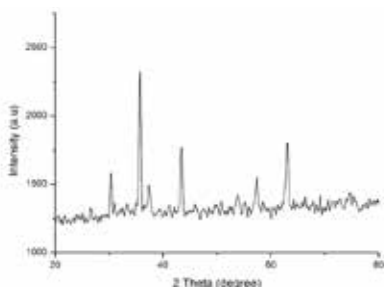


Fig.2 XRD pattern of the as-synthesized $\text{Ni}_{0.8}\text{Mn}_{0.2}\text{Fe}_2\text{O}_4$ nanoparticles

Morphology analysis

The microstructure plays an important role in realizing many application-oriented ferrite properties. Fig. 3a at higher magnification provides immense evidence for the presence of agglomerated worms like nanosized particles with a narrow distribution.

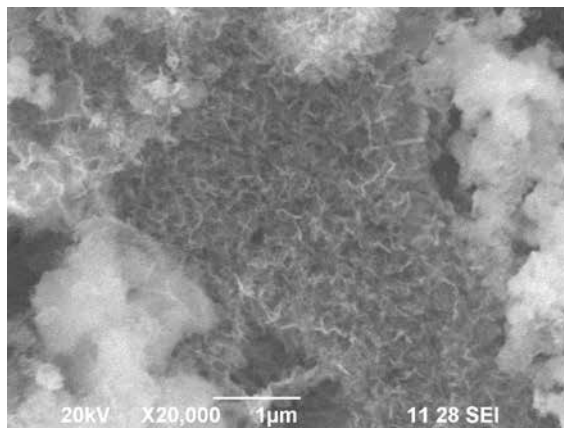


Fig.3a SEM image of the as-synthesized $\text{Ni}_{0.8}\text{Mn}_{0.2}\text{Fe}_2\text{O}_4$ nanoparticles

In order to confirm the chemical composition, EDX analysis was carried out and is shown in fig. 3b. This compositional analysis method results comply with what is expected from the synthesis. The result from EDX spectrum shows that the as-prepared $\text{Ni}_{0.8}\text{Mn}_{0.2}\text{Fe}_2\text{O}_4$ nanospheres contain Ni, Mn, Fe and O, and no contamination element was detected, indicating that the chemical formula of the as-prepared sample is consistent with the experimental stoichiometry.

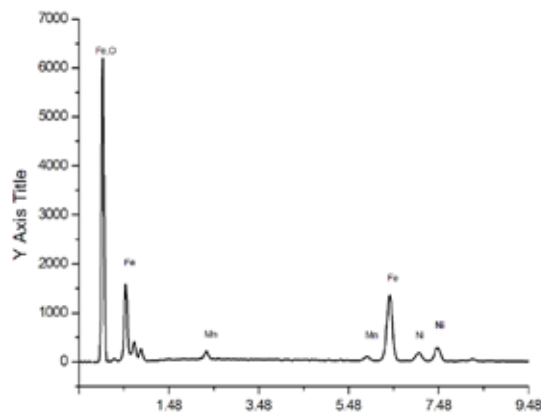


Fig.3b SEM EDX of as-synthesized $\text{Ni}_{0.8}\text{Mn}_{0.2}\text{Fe}_2\text{O}_4$ nanoparticles

Structural analysis

The size and morphology of the as-produced sample in detail were investigated by HRTEM. High resolution transmission electron microscopy (HRTEM) images (Fig. 4(a&b)) of $\text{Ni}_{0.8}\text{Mn}_{0.2}\text{Fe}_2\text{O}_4$ shows that the obtained nano particles were almost spherical, ultrafine and homogeneously dispersed with agglomeration. From fig.4b the crystallographic orientation of the $\text{Ni}_{0.8}\text{Mn}_{0.2}\text{Fe}_2\text{O}_4$ nanoparticles was investigated and the prominence of the lattice fringes was found to agree well with the separation between the lattice planes. The particle size calculated by HRTEM micrography was in the range of $9-17\text{ nm}$, which is in agreement with that calculated using the Debye-Scherrer formula.

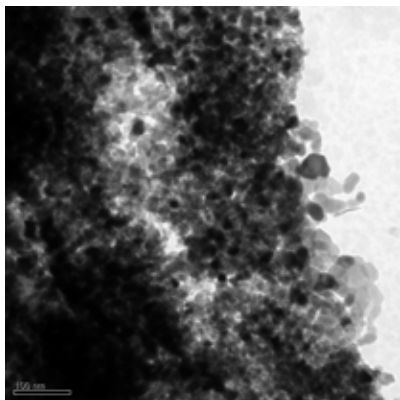


Fig.4a Tem image of as synthesized $\text{Ni}_{0.8}\text{Mn}_{0.2}\text{Fe}_2\text{O}_4$ nanoparticles

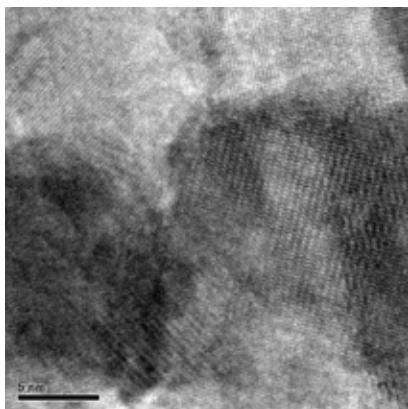


Fig.4b Tem image of as synthesized $\text{Ni}_{0.8}\text{Mn}_{0.2}\text{Fe}_2\text{O}_4$ nanoparticles

The electron diffraction pattern from the HRTEM image (Fig. 5) shows multiple diffraction rings, indicating crystalline structure formation. A careful analysis of the SAED pattern reveals that besides the diffraction rings of $\text{Ni}_{0.8}\text{Mn}_{0.2}\text{Fe}_2\text{O}_4$, no additional rings were observed. The bright electron diffraction rings for

$\text{Ni}_{0.8}\text{Mn}_{0.2}\text{Fe}_2\text{O}_4$ nanoparticles showed that the particles are fine nanocrystalline and are around 13 nm size.

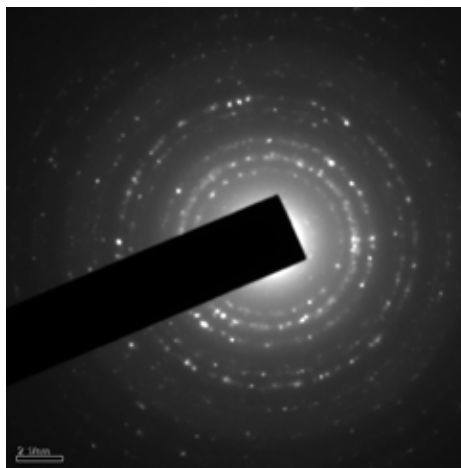


Fig.5 SAED pattern of the as-synthesized $\text{Ni}_{0.8}\text{Mn}_{0.2}\text{Fe}_2\text{O}_4$ nanoparticles

CONCLUSION

In summary, $\text{Ni}_{0.8}\text{Mn}_{0.2}\text{Fe}_2\text{O}_4$ nanoparticles were synthesised by thermal decomposition of the precursor complex $\text{Ni}_{0.8}\text{Mn}_{0.2}\text{Fe}_2(\text{PhAc})_3(\text{N}_2\text{H}_4)_5$ at room temperature. The unidentate coordination nature of the carboxylate ions and the bidentate coordination behaviour of hydrazine moieties were confirmed by the $\nu_{\text{asymm}} - \nu_{\text{symm}}$ value of 205 cm^{-1} and N-N stretching frequency at 977 cm^{-1} respectively. Thermal studies of the precursor complex showed a multi step degradation to form the corresponding oxide nanoparticles, the cubic spinel structure of which is confirmed by XRD studies. The average particle size of 13 nm determined by HRTEM is in agreement with that calculated using the Debye-Scherrer formula.

Thus, this novel route gives an efficient method of preparation of $\text{Ni}_{0.8}\text{Mn}_{0.2}\text{Fe}_2\text{O}_4$ nanoparticles, involving low cost, low energy, high purity, high nanocrystallinity and eco friendliness.

REFERENCE

- [1] Li e JG, Sun XD (2000) Synthesis and sintering behavior of a nanocrystalline alpha-alumina powder. ACT MATER. 48(12): 3103-3112 | [2] Al-Hilli M, Li SS, Kassim, K (2009) Microstructure, electrical properties and Hall coefficient of europium-doped Li-Ni ferrites. Materials Science and Engineering B. 158:1- 6 | [3] Ghazanfar U, Siddiqi SA, Abbas G (2005) Study of Room Temperature DC Resistivity in Comparison with Activation Energy and Drift Mobility of Ni-Zn Ferrites. Materials Science and Engineering B. 118:132-134 | [4] Gu M, Liu GQ, Wang W (2009) Study of Mn3O4 doping to improve the magnetic properties of MnZn ferrites. Materials Science and Engineering B. 158:35-39 | [5] McMichael RD, Shull RD, Swartzendruber IJ, Bennett LH (1992) Magnetocaloric effect in superparamagnets. J. Magn. Magn. Mater. 111:29-33 | [6] Ghasemi A, Hossienpour A, Morisako A, Saakhi A, Saleki M (2006) Electromagnetic properties and microwave absorbing characteristics of doped barium hexaferrite. J. Magn. Magn. Mater. 302: 429-435 | [7] Sahoo Y, Cheon M, Wang S, Luo H, Furlani EP Prasad PN (2004) Field-Directed Self-Assembly of Magnetic Nanoparticles. J. Phys. Chem. B. 108:3380-3383 | [8] Zhong L, Zhongwen L, Yu Z, Sun K, Ji H (2007) Influence of quencher on microstructure and magnetic properties of manganese-zinc ferrites. J. Magn. Magn. Mater. 318:39-43 | [9] Bonini M, Wiedenmann A, Baglioni P (2004) Synthesis and characterization of surfactant and silica-coated cobalt ferrite nanoparticles. Physica A. 339:86-91 | [10] Wang HW, Kung SC (2004) Crystallization of nanosized Ni-Zn ferrite powders prepared by hydrothermal method. J. Magn. Magn. Mater. 270:230-236 | [11] Liu XM, Fu SY, Huang CJ (2004) Magnetic properties of Ni ferrite nanocrystals dispersed in the silica matrix by sol-gel technique. J. Magn. Magn. Mater. 281:234-239 | [12] Chander S, Srivastava BK, Krishnamurthy A (2004) Magnetic behaviour of nano-particles of $\text{Ni}_0.3\text{Co}_0.5\text{Fe}_2\text{O}_4$ prepared using two different routes. Indian J. Pure and Appl. Phys. 42:366-370 | [13] Porob RA, Khan SZ, Mojumdar SC, Verenker VMS (2006) Synthesis, TG, DSC and infrared spectral study of $\text{NiMn}_2(\text{C}_4\text{H}_4\text{O}_4)_3 \cdot 6\text{N}_2\text{H}_4$: A precursor for NiMn_2O_4 nanoparticles. J. Therm. Anal. Cal. 86:605-608 | [14] More A, Mojumdar SC, Parab S, Verenker VMS. Preparation, purification and characterisation of nanoparticle ferrite from novel fumarato-hydrazinate precursor: 15 th CTAS Annual Workshop and Exhibition, | [15] Gajapathy D, Patil KC, Pai Vernekar VR(1982) Low temperature ferrite formation using metal oxalate hydrazinate precursor: Mater Res Bull. 17(1):29-32 | [16] Randhawa BS, Kaur S, Bassi PS(1999) Thermal decomposition of strontium and barium malonates. J Therm Anal Calorim. 55(3):789-796 | [17] Randhawa BS, Dosanji HS, Kumar N (1999) Synthesis of potassium ferrite by precursor and combustion methods a comparative study. J Therm Anal Calorim. 95(1):75-80 | [18] Sivasankar BN (2006) Cobalt(II), nickel(II) and zinc(II) dicarboxylate complexes with hydrazine as bridged ligand characterization and thermal degradation. J Therm Anal Calorim. 86(2):385-392 | [19] Sivasankar BN, Govindraj S (1997) Acetate and malonate complexes of cobalt(II), nickel(II) and zinc(II) with hydrazinium cation: preparation, spectral and thermal studies. J Therm Anal. 48(6):1401-1413 | [20] Rane KS, Verenkar VMS (2001) Synthesis of ferrite grade c-Fe2O3. Bull Mater. Sci. 24(1):39-45 | [21] Randhawa BS, Kaur M (2007) A comparative study on the thermal decomposition of some transition metal maleates and fumarates. J Therm Anal Calorim. 89(1):251-255 | [22] Khalil I, Petit-Ramel MM (1979) Polynuclear complexes quantitative and qualitative study of copper-yttrium malate and copper-uranyl malate. J Inorg Nucl Chem. 41(5):711-716 | [23] Gawas UB, Mojumdar SC, Verenkar VMS (2009) $\text{Ni}_0.5\text{Mn}_0.1\text{Zn}_0.4\text{Fe}_2(\text{C}_4\text{H}_2\text{O}_4)_3 \cdot 6\text{N}_2\text{H}_4$ precursor $\text{Ni}_0.5\text{Mn}_0.1\text{Zn}_0.4\text{Fe}_2\text{O}_4$ nanoparticles preparation, IR spectral, XRD, SEM-EDS and thermal analysis. J Therm Anal Calorim. 96(1):49-52 | [24] Gonsalves LR, Verenkar VMS, Mojumdar SC (2009) Preparation and characterization of $\text{Co}_0.5\text{Zn}_0.5\text{Fe}_2(\text{C}_4\text{H}_2\text{O}_4)_3 \cdot 6\text{N}_2\text{H}_4$: a precursor to prepare $\text{Co}_0.5\text{Zn}_0.5\text{Fe}_2\text{O}_4$ nanoparticles. J Therm Anal Calorim. 96(1):53-57 | [25] More A, Verenkar VMS, Mojumdar SC (2008) Nickel ferrite nanoparticles synthesis from novel fumarato-hydrazinate precursor. J Therm Anal Calorim. 94(1):63-67 | [26] Vogel I (1986) A Text Book of Quantitative Inorganic Analysis, 4th Ed., Longman: London | [27] Nakamoto K (1962) Infrared spectra of inorganic and coordination compounds, second ed., Wiley & sons: New York | [28] Braibanti A, Dallavalle F, Pellinghelli MA, Leporati E (1968) The nitrogen-nitrogen stretching band in hydrazine derivatives and complexes. Inorg. Chem.7:1430-1433 | [29] Pandit AA, More SS, Dorik RG, Jadhav KM (2003) Structural and magnetic properties of $\text{Co}_1+\text{y}\text{Ni}_y\text{Fe}_2-2\text{y-x}\text{Cr}_x\text{O}_4$. Bull. Mater. Sci. 26(5): 517-521 | [30] Akther Hossain AKM, Mahmud ST, Seki M, Kawai T, Tabata H (2007) Structural, electrical transport, and magnetic properties of $\text{Ni}_1-x\text{Zn}_x\text{Fe}_2\text{O}_4$. J Magn Magn Mater. 312(1):210-219 | [31] Zhou L, Cui Y, Hua Y, Yu L, Jin W, Feng S (2006) The magnetic properties of $\text{Ni}_0.7\text{Mn}_0.3\text{GdxFe}_2-x\text{O}_4$ ferrite Mater. Lett. 60:104-108 | [32] George M, John AM, Nair SS, Joy PA, Anantharaman F (2006) Finite size effects on the structural and magnetic properties of sol-gel synthesized NiFe_2O_4 powders. J. Magn. Magn.Mater. 302(1):190-195 |